Earthquake Engineering, Tenth World Conference © 1992 Balkema, Rotterdam. ISBN 90 5410 060 5

Probing characteristics of vertical strong motions

Yoshihiko Akao
Shimizu Corporation, Tokyo, Japan
Seiichiro Fukushima & Mamoru Mizutani
Tokyo Electric Power Services Co., Japan

ABSTRACT: Statistic properties of vertical strong ground motions from near-field earthquakes are discussed in comparison with that of horizontal motions. It is a feature of this research that time history of each observed record is divided into a few segments from a seismological viewpoint. Following results are obtained. Vertical-motion energy excited by direct S-waves is about 0.6 times of horizontal ones at deep underground, and it approaches to 1.0 at shallow place. Meanwhile, horizontal-motion energy excited by direct P-waves become 0.2 times(at deep) or more(at shallow) of vertical one. These results would be available for modeling of input motions for aseismic design.

1. INTRODUCTION

To reduce seismic risks, it is an emergency problem in the earthquake engineering to probe characteristics of vertical motions. Especially, both are important for aseismic design, that defining a relationship of vertical component and horizontal component in strong motion records, and that strong vertical accelerations more than the earth gravity occasionally happen in the seismic source region. In this paper, we deal with the former problem. The later problem was discussed in the other paper (Akao 1991).

Conventionally, the whole duration of a strong motion record (i.e., from the first datum to the last datum) has been used to investigate characteristics of vertical motions as well as many other engineering analyses. However, a strong motion record consists of several kinds of seismic waves (i.e., direct P-wave, direct S-wave, reflected wave, surface wave). Different-kind waves should show different behavior, different amplification, and different energy from each other. It is not appropriate to discuss about characteristics of strong motions simply based on time-history records without discrimination of their causal waves.

In this study, direct P-wave and direct S-wave segments are identified from the record, and characteristics of each wave segment is investigated. We designate this method "segmentation approach". The first idea of the segmentation approach has been imported form the seismology to the earthquake engineering by one of the author (Anderson and Akao 1985).

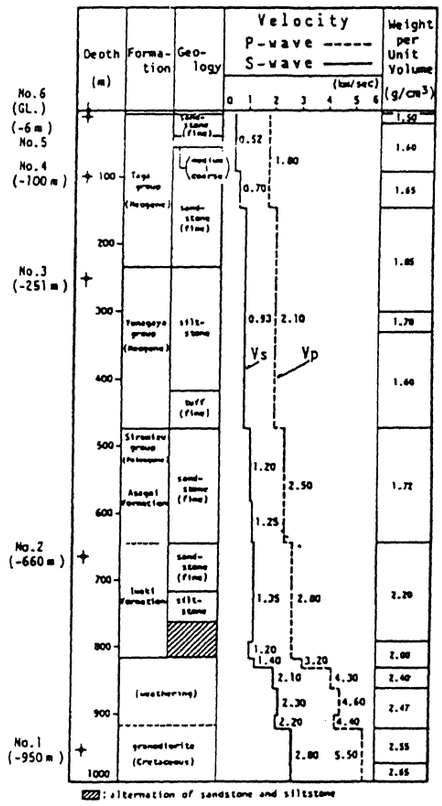

Fig. 1. Location of seismograph and ground properties. (After Omote et al. 1984)

A. P- and S-wave durations could be identified

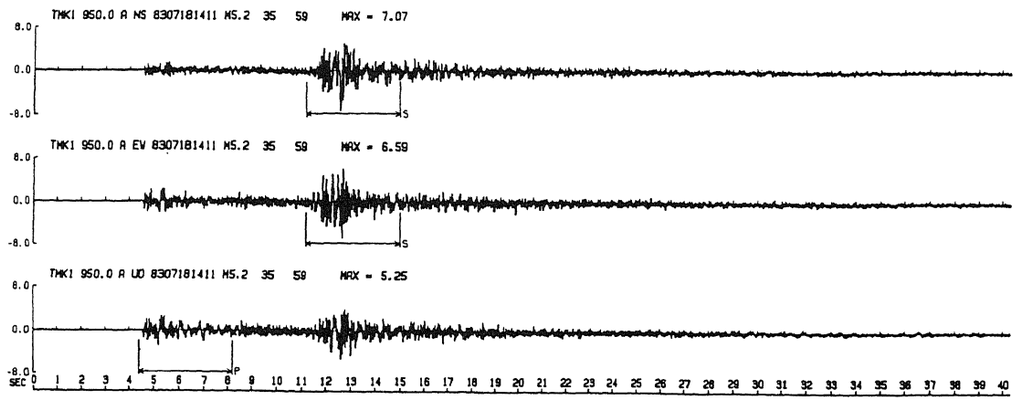

B. Only S-wave duration could be identified

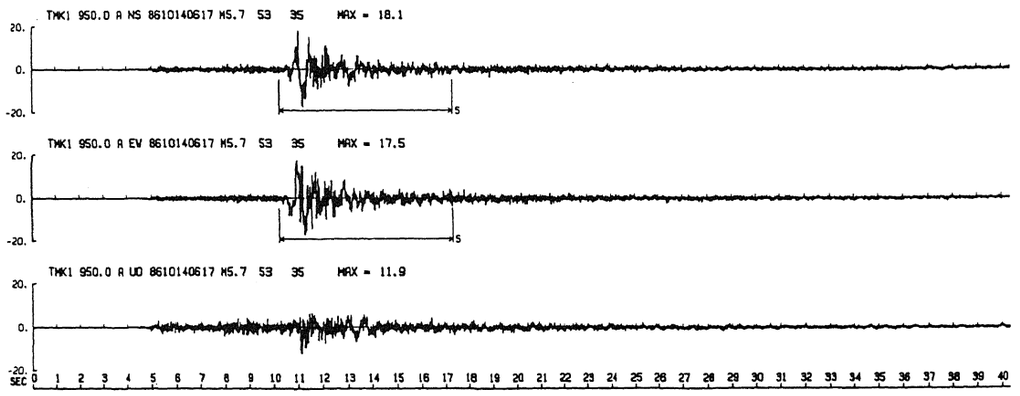

C. Any direct-wave duration could not be distinguished

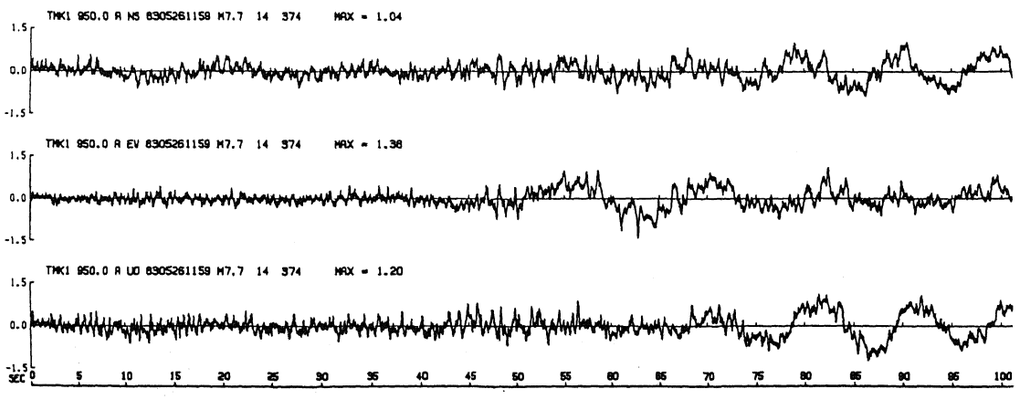

Fig. 2. Three typical waveforms observed at GL-950m.

2. OBSERVATION AND RECORDS

The purpose of this study is to investigate feature of the strong motion records from observation network under the ground. The observation station, Tomioka, Eastern Japan, which lies on a hard rock with thin alluvium as shown in Fig. 1, is selected to apply to the analysis. Several seismographs ranging from the ground surface to a deep basement rock along a vertical axis are distributed at this station. We employed the five acceleration seismographs of them, namely at the ground surface, GL-100m, GL-250m, GL-250m, GL-660m, GL-950m.

In this study only direct-wave segments are adopted for the analysis. The segments are identified by looking at waveforms as shown in Fig. 2. Waveforms of the all records can be classified to three kinds of types. In the first typical seismogram as shown on the upper figure, direct P- and S-wave segment could be identified. The recorder of the observation system equips 10-seconds delay circuit, then first weak tremor(P-wave motion) prior to major tremor (S-wave motion) can be recorded. In the second typical seismogram as shown on the middle, only S-wave segment could be identified either because of that the recorder failed recording P-wave motion, or that first tremor was too weak to identify the P-wave motion. The other seismogram, as shown on the lower, could not identify any direct wave duration. Noisy records are excluded in this type.

It is not meaningless to examine a cause of the difference of these seismograms. After a few examinations, the cause could be concluded that the difference depends mainly on relation between focal depths and epicentral distances. Generally to say, waveforms from shallow large earthquakes are complex and hard to find any direct-wave phases. Waveforms from relatively deep earthquakes comparing with their epicentral distances could identify direct wave durations. Then, identified segments are thought to be excited by direct waves and not to include any reflective or refractive waves.

3. METHOD TO PROBE CHARACTERISTICS

As shown Fig. 3, ray paths of the direct waves incline to upper direction among near surface layers due to low wave velocities. Then, the P-wave motions are thought to be dominant on vertical direction to horizontal direction, while the S-wave motions are thought to be dominant on horizontal direction to vertical direction.

Energy spectrum '$S_{XX}(\omega)$' of major components in P-wave or S-wave segments will be discussed in the following section. Amplitude ratio $R_{XY}(\omega)$ and coherence $C_{XY}(\omega)$ between vertical and horizontal components will also be compared for each segment. These spectral functions are defined as followings. Let $u_V(t)$ be time history of vertical motion, and let $u_h(t)$ be that of horizontal motion. Cross spectrum $S_{XY}(\omega)$ is defined as following,

$$S_{XY}(\omega)=U_Y(\omega)\cdot U_X^*(\omega).$$

$U_X(\omega)$ is a Fourier Spectrum of $u_X(t)$, which is a major component of either $u_V(t)$ or $u_h(t)$. $U_Y(\omega)$ is that of $u_Y(t)$, which is a minor component. Asterisk '*' indicates the conjugate. Energy spectrum $S_{XX}(\omega)$ is obtained by replacing $U_Y(\omega)$ by $U_X(\omega)$. Amplitude ratio $R_{XY}(\omega)$ and coherence $C_{XY}(\omega)$ can be written as,

$$R_{XY}(\omega)=S_{YY}(\omega)/S_{XX}(\omega),$$

$$C_{XY}(\omega)=|S_{XY}(\omega)|/(S_{XX}\cdot S_{YY}).$$

S_{XX}, S_{YY}, S_{XY}, are normalized by total energy of S_{XX} due to correcting difference of amplitude of each record. Besides it, we employed ensemble average of the all available cross spectra as '$S_{XY}(\omega)$'.

4. NUMERICAL RESULTS

Energy spectrum $S_{XX}(\omega)$ of P-wave and S-wave motion observed at the surface, GL-250m, GL-950m are shown in Fig. 4. Considerably distinct ripples are found in the spectra of GL-250m. These spectral shapes are thought to be caused by reflective waves. In homogeneous half space, the reflective waves go down from the ground surface without being confused by the surface layers. When phase delay time of reflective wave corresponds to oscillational period of incident wave, underground tremor would be amplified. On the other hand when phase delay time corresponds to half time of oscillational period, underground tremor would vanish by canceling. Amplification and canceling would appear periodically.

Let t_i be two-ways time (intercept time) during which seismic waves come up and go

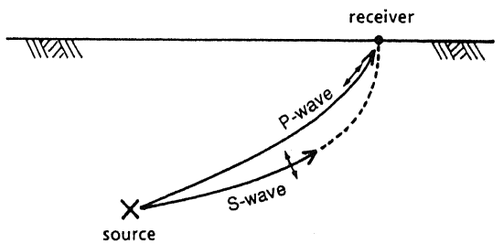

Fig. 3. Ray paths of directly propagating P-wave and S-wave, and their oscillational directions.

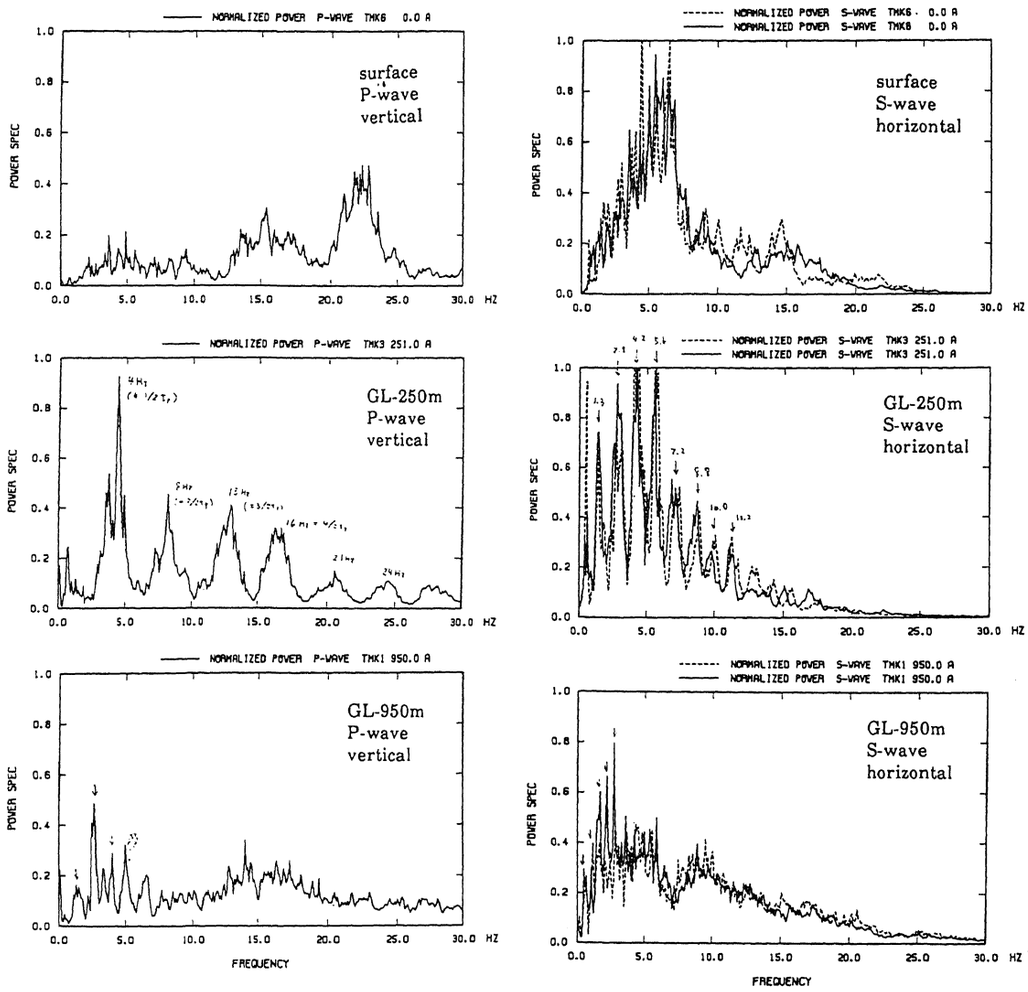

Fig. 4. The energy spectra of the major components of both segments, which are regarded as P-wave and S-wave motions, are indicated.

down between an observation point underground and the surface as shown in Fig. 5. An amplitude of observed motion which has a frequency n/t_i(n=1, 2, 3, ···) is magnified two times of incident wave. Meanwhile, an amplitude of observed motion of frequencies $(2n-1)/2t_i$(n=1, 2, 3, ···) vanishes. The intercept time calculated from velocity structure and predominant periods read from spectral peaks are compared in Table 1. Spectral ripples on energy spectra also appear at other points, but those at GL-250m are the strongest among all points. From these results we can conclude that the data upper than GL-660m are strongly affected by reflective waves.

The amplitude ratio $R_{xy}(\omega)$ of both segments recorded at the surface and GL-950m

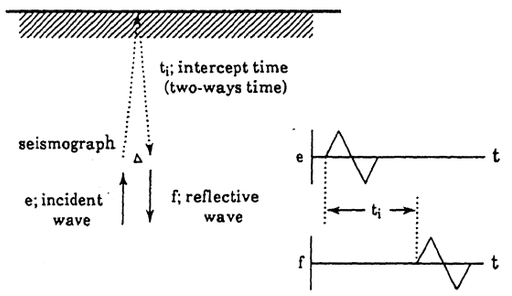

Fig. 5. Schematic relation of incident wave motion and reflective wave motion under the ground.

are shown in Fig. 6. Mean ratio averaged between 1Hz and 30Hz are indicated by bold lines. In general, the ratio is small at the deep and increased close to 1.0 at the surface. The ratio of P-wave is smaller than of S-wave.

Considering variation of ray-path trend, the ratios of two components of direct waves should increase with depth, and should be smaller for S-wave than P-wave. The observed results are inconsistent with these consideration. Then, we propose a schematic model that observed motion is consisting of direct-wave signal D(t) and noise rate N(t).

$$u_X(t)=D_X(t)+N(t)$$

$$u_Y(t)=D_Y(t)+N(t)$$

The noise rate N(t), which is assumed to be equal in any direction, decreases with depth, and it is larger for S-wave than P-wave. Two reasons are considered that noise generation is more exciting at the surface, and that S-wave segment is including coda waves more than P-wave segment.

The coherences $C_{XY}(\omega)$ at the surface and GL-950m are also shown in Fig. 7. It is important for seismic resistant design whether any connections between horizontal components and vertical components is existing. However, available relation between horizontal components and a vertical component could not be recognized, especially for S-wave segments. Neither could be it at the other positions. If we design a seismic load model, it will not be necessary to consider maximum horizontal load and maximum vertical load simultaneously.

5. CONCLUSION

In this study, the characteristics of vertical components of strong motions are investigated, and following results are obtained.

1. Amplitude rate of vertical motion due to a direct P-wave is more than 2-times of horizontal motion in average.

2. Ratio of vertical motion rate due to a direct S-wave to horizontal one is about 0.6 at the deep underground, and approaches to 1.0 at the surface.

3. These ratio of two components could be explained by the signal-noise combination model.

4. Any available relation between a vertical component and a horizontal component for each direct-wave segment is not recognized.

Thus, we revealed feature of strong motions to some extent. It can be concluded that the segmentation approach is useful not only to identify the characteristics of vertical motions but also to understand the strong motions themselves.

ACKNOWLEDGMENTS: The acceleration data were made available by "Research Committee on Earthquake Obser-vation with Vertical Instrument Array in Rock" (chairmana Prof. S.Omote)

REFERENCE

Akao,Y.(1991). Subject on intense vertical component of earthquake ground motion exceeding the gravity acceleration, Proc. of Jap.Soc.Civil Eng. No.432/I-16.

Anderson,J.G. and Y.Akao(1985). Spectral attenuation of underground observation records, Proc. of Seismological Soc.Jap.

Omote,S. et al.(1984) Observation of Earthquake Strong-Motion with Deep Boreholes -An Introductory Note for Iwaki and Tomioka Observation Station in Japan-, Proc. of 8th WCEE.

Table 1. Comparison of the intercept time calculated from the ground structure and the peak frequencies picked up from the observed spectra.

position	P-wave intercept	dominant frequency (Hz)	S-wave intercept	dominant frequency (Hz)
GL-100m	t_i = 0.31 s [f_1 = 3.2Hz]	no id	t_i = 0.40 s [f_1 = 2.5Hz]	3, 5.5, 8 [t_i = 0.37 s]
GL-250m	t_i = 0.31 s [f_1 = 3.2Hz]	4, 8, 13, 16, 21, 24 [t_i = 0.25 s]	t_i = 0.76 s [f_1 = 1.3Hz]	1.3, 2.8, 4.2, 5.6, 7.2, 8.8, 10, 11.2 / [.72 s]
GL-660m	t_i = 0.67 s [f_1 = 1.5Hz]	1.9, 3.4, 4.7, 6.6, 8.3, 9.7 / [t_i = 0.62 s]	t_i = 1.54 s [f_1 = .65Hz]	0.7, 1.2, 1.9, 2.7, 3.3 [t_i = 1.5 s]
GL-950m	t_i = 0.84 s [f_1 = 1.2Hz]	1.3, 2.6, 4 [t_i = 0.75 s]	t_i = 1.90s [f_1 = .52Hz]	hard to find

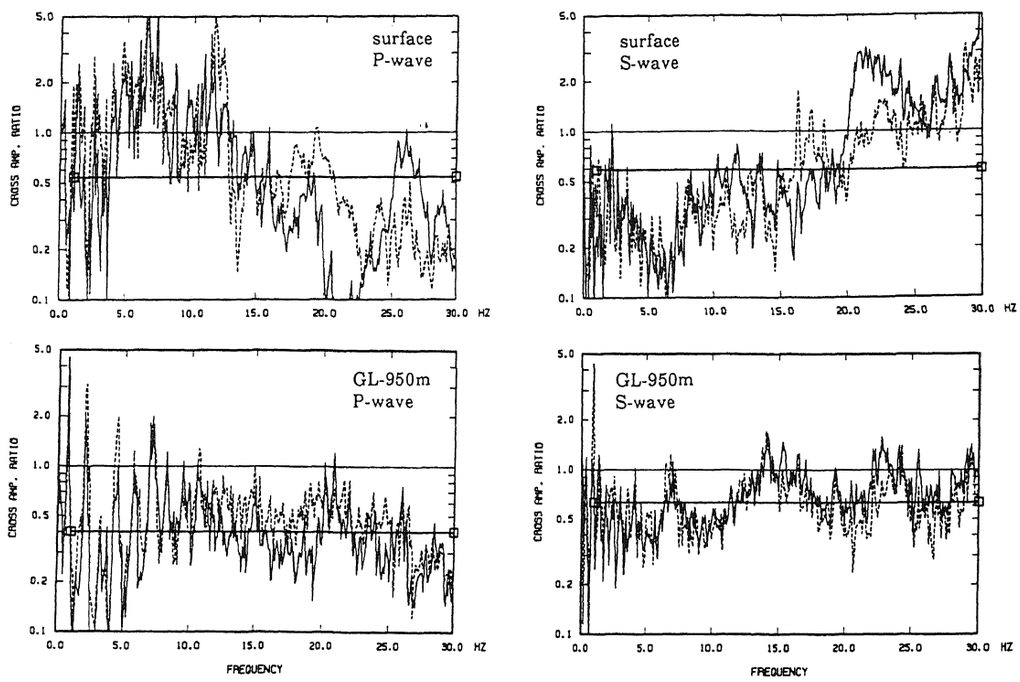

Fig. 6. The spectral ratio of the minor component energy against the major one.

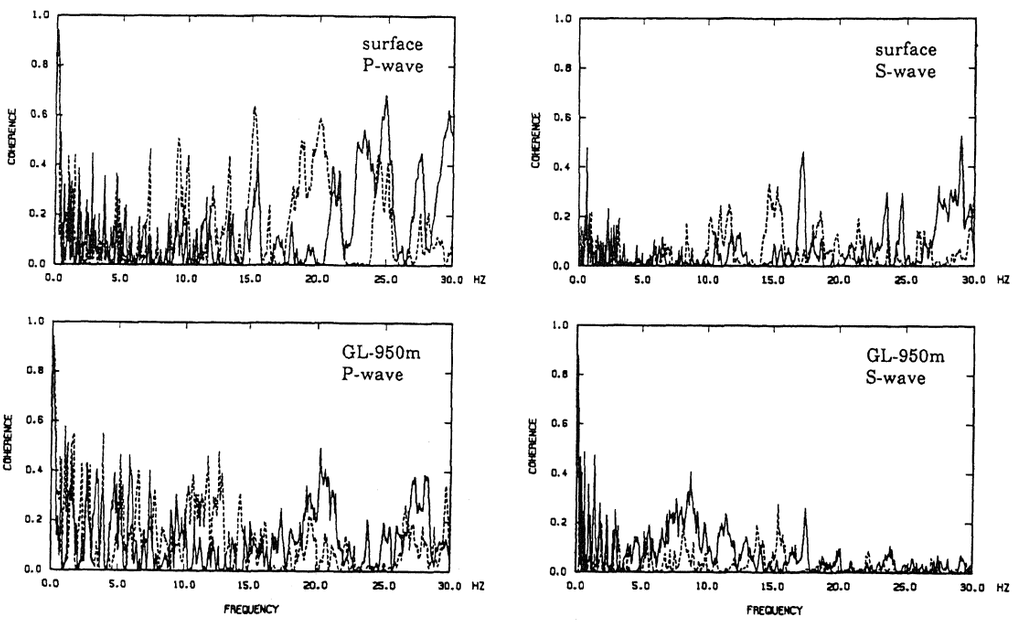

Fig. 7. The coherence between vertical component and horizontal component for P-wave and S-wave segments.